First Direct Observation of Runaway-Electron-Driven Whistler Waves in Tokamaks

D. A. Spong,[1] W. W. Heidbrink,[2] C. Paz-Soldan,[3] X. D. Du,[2] K. E. Thome,[4] M. A. Van Zeeland,[3] C. Collins,[3] A. Lvovskiy,[4] R. A. Moyer,[5] M. E. Austin,[6] D. P. Brennan,[7] C. Liu,[7] E. F. Jaeger,[8] and C. Lau[1]

[1]*Oak Ridge National Laboratory, Oak Ridge, Tennessee 37831, USA*
[2]*University of California—Irvine, Irvine, California 92697, USA*
[3]*General Atomics, San Diego, California 92186-5608, USA*
[4]*Oak Ridge Associated Universities, P.O. Box 117, Oak Ridge, Tennessee 37831, USA*
[5]*University of California—San Diego, La Jolla, California 92093, USA*
[6]*University of Texas, Austin, Texas 78705, USA*
[7]*Princeton Plasma Physics Laboratory, Princeton, New Jersey 08543, USA*
[8]*XCEL Engineering, Oak Ridge, Tennessee 37830, USA*

(Received 8 December 2017; published 11 April 2018)

DIII-D experiments at low density ($n_e \sim 10^{19}$ m^{-3}) have directly measured whistler waves in the 100–200 MHz range excited by multi-MeV runaway electrons. Whistler activity is correlated with runaway intensity (hard x-ray emission level), occurs in novel discrete frequency bands, and exhibits nonlinear limit-cycle-like behavior. The measured frequencies scale with the magnetic field strength and electron density as expected from the whistler dispersion relation. The modes are stabilized with increasing magnetic field, which is consistent with wave-particle resonance mechanisms. The mode amplitudes show intermittent time variations correlated with changes in the electron cyclotron emission that follow predator-prey cycles. These can be interpreted as wave-induced pitch angle scattering of moderate energy runaways. The tokamak runaway-whistler mechanisms have parallels to whistler phenomena in ionospheric plasmas. The observations also open new directions for the modeling and active control of runaway electrons in tokamaks.

DOI: 10.1103/PhysRevLett.120.155002

Introduction.—Whistler instabilities have been measured for many years in natural plasmas [1,2], such as Earth's ionosphere and Van Allen belts, where they are driven by energetic electrons [3] injected either by lightning strikes, or solar substorms. Ionospheric whistlers play an important role in the variability of Earth's radiation belts [4–6]. The excitation of whistler instabilities in laboratory plasmas [7,8] can provide a more controlled environment for understanding the underlying physical mechanisms. Runaway driven whistler instabilities have been studied [9,10] for ITER and existing experiments; also, strong runaway-related instabilities were reported in early tokamak experiments [11,12]. In this Letter the first direct measurements of relativistic (runaway) electron driven whistler instabilities in a tokamak plasma are reported. Runaway electrons can be created in the tokamak at startup by the induction electric field used to drive the toroidal plasma current [13,14], or transiently by the electric fields from disruptive instabilities, leading to runaway avalanches [15] in devices with sufficient plasma current. In either case, once electrons achieve a velocity where collisional drag forces are less than the electric field acceleration, they freely accelerate to higher energies, until limited by synchrotron radiation damping [16] or instabilities. Such runaways can form a significant hazard to plasma-facing components, and much effort is focused on mitigation of their effects, especially in the case of future devices, such as ITER [17]. The whistler wave instabilities described in this Letter are important for extending whistler physics to new regimes, improving the understanding of runaway physics, and developing new methods to prevent their acceleration to high energies.

This Letter demonstrates the controlled excitation of whistler waves in a tokamak plasma, and describes several new features not seen in other settings. First, the whistler frequency spectra show a unique structure, consisting of multiple, coherent lines. This is likely caused by individual eigenmodes related to the bounded, periodic nature of the tokamak plasma, but wave cutoff, damping effects or scattering off other plasma waves are also possible causes. Second, stability boundaries are observed that depend on the density and energy of the relativistic electrons and on the magnetic field strength. In common with ionospheric whistlers, the tokamak whistlers are expected to lead to pitch angle scattering of energetic electrons. The measured wave amplitudes display intermittency, which can be attributed both to a scattering of runaways by whistler waves and to periodic magnetic relaxation oscillations (involving fast magnetic reconnections, also known as sawteeth). This observed runaway scattering opens up the intriguing possibility that runaways in a tokamak could be mitigated by the intentional launching of whistlers. Instability induced scattering may also play a role in discrepancies seen between observed runaway electric field thresholds and predictions [18].

Experiment and diagnostics.—The whistler experiments were performed on the DIII-D tokamak device in very low density Ohmic plasmas [19–21]. DIII-D is a D-shaped cross section tokamak with major radius $R_0 = 1.7$ m, minor radius $\langle a \rangle = 0.6$ m. Magnetic fields were varied from 1 to 1.9 T and densities from $n_e(0) = 0.5$ to 1×10^{19} m^{-3} were used. In these conditions, an initial runaway population is created by the Ohmic electric field while the plasma density is reduced. As the runaways reach a prespecified intensity level, a gas puff is triggered to begin the dissipation phase. A runaway beam is generated with energies up to about 20 MeV. The whistler fluctuations were associated with the presence of these runaway beams and measured using magnetic signals from fast-wave antenna straps and toroidal rf loops located on the outboard side of the tokamak. CO_2 interferometric plasma density fluctuation measurements were also active, but did not show any fluctuations in the whistler frequency range.

Frequency spectra and dispersion relation.—In Fig. 1, the evolving frequency spectra and parameters associated with a typical runaway discharge are shown. Multiple discrete modes at frequencies ranging from 120 to 160 MHz become evident at $t \sim 3.5$ sec; these gradually drop to lower frequencies as the plasma density rises and the magnetic field strength decreases.

The parametric behavior of the frequency can be understood from the cold plasma dispersion relation as given below.

$$\omega = k \mathrm{V}_A \sqrt{1 + k_\parallel^2 c^2 / \omega_{pi}^2}, \tag{1}$$

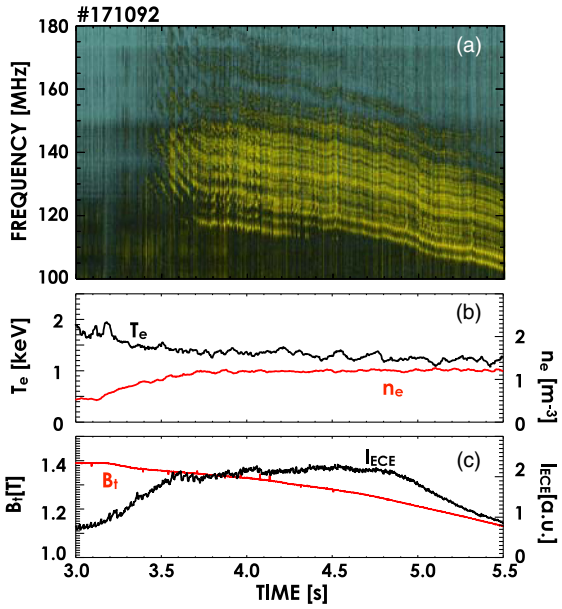

FIG. 1. Time evolution of (a) the magnetic fluctuation power spectra; (b) the electron temperature (T_e); electron density (n_e); and (c) the toroidal magnetic field (near the magnetic axis), and ECE—a measure of runaway perpendicular energy.

where v_A = Alfvén velocity, ω_{pi} = ion plasma frequency, and k = wave number. Here the kinetic runaway contribution is neglected; while important for stability, it is expected to only have a minor (perturbative) effect on the whistler wave real frequency. To lowest order Eq. (1) would predict a linear scaling of the frequency with the magnetic field strength ($\omega \propto B$) and an inverse square root scaling ($\omega \propto n^{-1/2}$) with the plasma density. These scalings are consistent with the decreasing frequencies shown in Fig. 1. Figure 2 confirms these trends, including data from other discharges. In Fig. 2(a) a linear scaling with magnetic field strength (shown here in terms of the ion cyclotron frequency) is verified and Fig. 2(b) expands on the density scaling characteristics. Several different dependencies on plasma density are shown for different frequency lines.

Based on Eq. (1), the scaling with density should vary from $1/{n_e}^{1/2}$ (for $k_\parallel^2 c^2/\omega_{pi}^2 \ll 1$) to $1/n_e$ (for $k_\parallel^2 c^2/\omega_{pi}^2 \gg 1$). The fits from Fig. 2(b) fall within these limits. The discrete nature of the observed frequencies has been analyzed using both MHD and warm plasma rf wave absorption models. The MHD equations can be reduced to a 2D eigenmode problem for the Alfvén frequency range ($\omega \sim k\mathrm{v}_A$); solutions indicate many discrete normal modes in the observed frequency range. Full wave solutions, taking into account warm plasma absorption at ion cyclotron harmonics, ion Landau, and electron Landau damping have been obtained with the AORSA model [22]; typical mode structures and a power absorption scan vs frequency are shown in Fig. 3. It is expected that whistler waves would be more readily destabilized at the minima of wave damping vs frequency [Fig. 3(b)]. The strong variation in the damping is related to

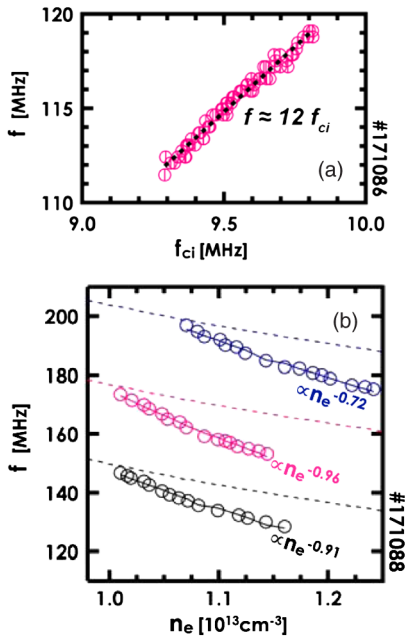

FIG. 2. (a) Variation of mode frequency at constant density with ion cyclotron frequency; (b) variation of mode frequency with electron density and fits (dashed lines are based on $f \propto n_e^{-1/2}$).

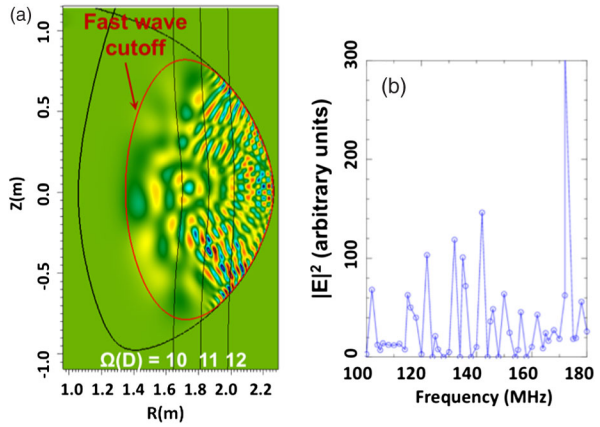

FIG. 3. (a) Wave electric field for toroidal mode number $n = 35$ at 140 MHz; (b) power absorption as a function of frequency.

the quantization condition of fitting an integral number of wavelengths within the fast wave cutoff region, which varies with frequency (cutoff density $\propto k_\parallel^2 B/\omega$). The resulting sequence of discrete cavity mode frequencies (power absorption minima) is consistent with the observations.

Runaway electron resonances and whistler stability thresholds.—Because of the collisional decoupling of the runaway component from the thermal plasma, the whistler destabilization is expected to occur via wave-particle resonances [9,10]. The instability drive can arise from spatial gradients, anisotropy, or positive velocity gradients, all of which can be present in runaway distributions. A general resonance condition for the coupling of relativistic electrons to whistler waves may be written as follows.

$$\omega - k_\parallel v_\parallel - k_\perp v_d - l\Omega_{ce}/\gamma = 0 \qquad (2)$$

where

$$v_d = \frac{\gamma}{\Omega_{ce}}\left(\frac{v_\perp^2}{2}\hat{b}\times\nabla\ln B + v_\parallel^2\hat{b}\times\kappa\right),$$
$$\gamma = (1 - v^2/c^2)^{-1/2}, \qquad \hat{b} = \mathbf{B}/|B|,$$
$$\kappa = (\hat{b}\cdot\nabla)\hat{b}, \qquad \Omega_{ce} = \frac{eB}{m_o},$$

and ω is the whistler wave frequency. Here l is an integer, but for the current purposes only $l = 0, \pm 1$ will be of interest. Taking Ω_{ce} as >0, the case $l = -1$ is denoted as the anomalous Doppler resonance, $l = 0$ is the Cherenkov resonance, and the case $l = +1$ will be referred to here as the normal Doppler resonance. This categorization is based upon $k_\parallel > 0$; if $k_\parallel < 0$, the sign of l should be reversed. The wave numbers $k_\parallel$ and k can be inferred by fitting the dispersion relation (1) to observations such as given in Figs. 2(a) and 2(b) where the magnetic field and plasma density were varied. This has indicated $k = 55$–80 m^{-1} and $\theta = 50°$–$70°$ (where $k_\parallel = k\cos\theta$) as likely ranges. Using these, the resonant frequencies can be evaluated from Eq. (2); typical results are shown in Fig. 4 as a function

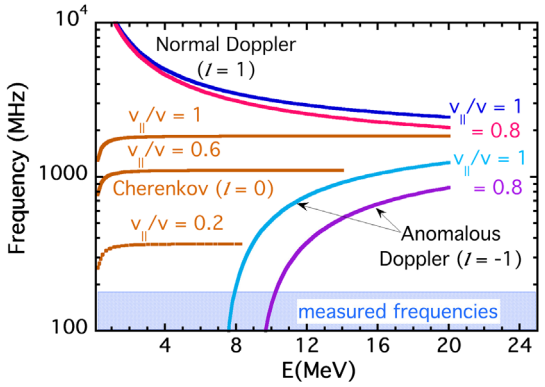

FIG. 4. Cherenkov, normal, and anomalous Doppler resonances for $B = 1$ T, $k = 60$ m^{-1}, and $\theta = 50°$ as a function of electron energy.

of energy and for several values of the runaway electron pitch angle parameter $v_\parallel/v$, which is expected to be in a range near 1 for runaways. As can be seen, the measured frequencies are intersected by the anomalous Doppler resonances, at higher runaway energies (>7 MeV). The Cherenkov and normal Doppler resonances are at higher frequencies, and cover both low and high energy ranges.

Since whistler waves can occur over a wide frequency range (from ion to electron cyclotron frequencies), all of the resonance branches shown in Fig. 4 can potentially be involved.

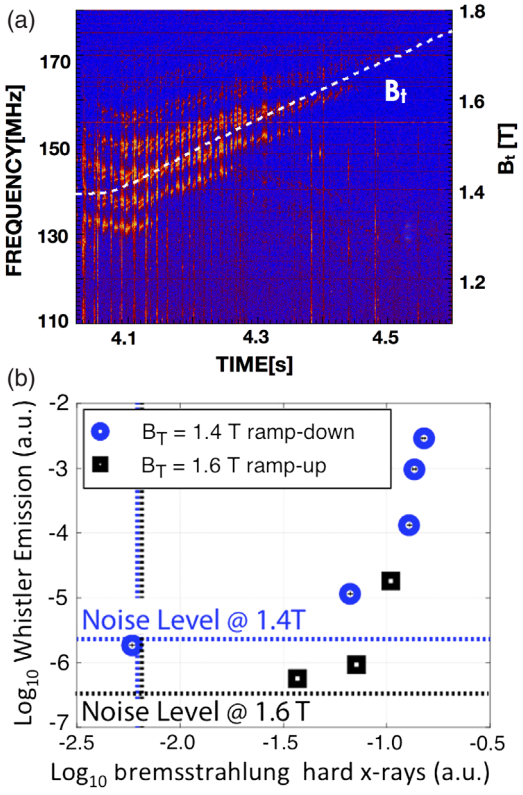

FIG. 5. (a) Decreasing whistler activity with increasing magnetic field; and (b) threshold in averaged whistler emission power vs hard x-ray bremsstrahlung level.

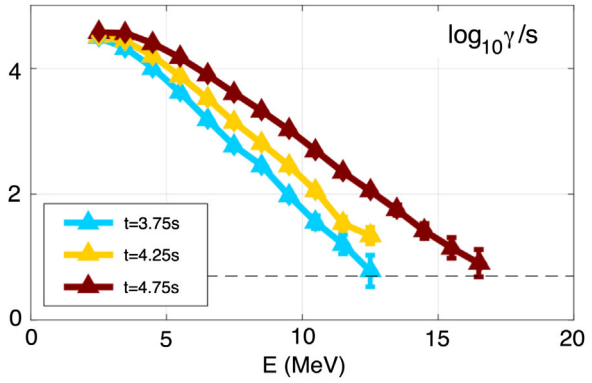

FIG. 6. Time evolution of runaway generated hard x-ray gamma energy spectrum for discharge No. 171089 of Fig. 5(a). Whistlers were present for $t = 3.75$, 4.25, and absent for $t = 4.75$ sec.

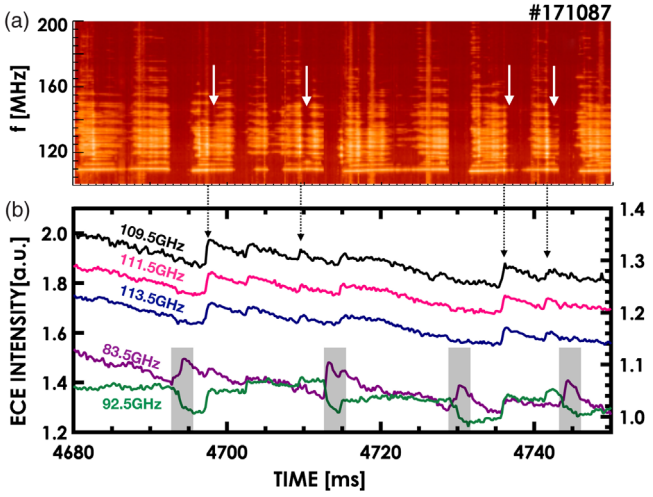

FIG. 7. Time evolution of (a) 100–200 MHz magnetic fluctuation power spectra; (b) ECE intensity at 83.5, 92.5, 109.5, 111.5, and 113.5 GHz. Dashed arrows in (b) are times at which the ECE and whistler amplitudes peak; solid arrows in (a) are times at which whistler amplitudes drop. The gray shaded bars are intervals of $n = 1$ sawtooth activity.

Figure 5 presents experimental evidence of whistler marginal stability boundaries. In Fig. 5(a) a sequence of whistlers is stabilized by increasing the magnetic field, starting at lower frequencies and propagating to higher frequencies. Figure 5(b) indicates a stability threshold in runaway intensity, as measured by hard x-ray levels. Whistler stability models [9,10] have attributed linear thresholds to collisional damping effects.

The successive stabilization of whistler frequency bands in Fig. 5(a) is roughly consistent with the anomalous Doppler resonance. As the magnetic field increases, the anomalous Doppler resonance shifts to higher energy. The measured energy spectrum of runaway-produced gammas is shown in Fig. 6 for several times in the discharge of Fig. 5(a), indicating an upper energy that increases in time (from ~12 to 17 MeV as time varies from 3.75 to 4.75 sec). This lags behind the resonant energy upshift (leading to stability for $B \gtrsim 1.6$ T) if one considers runaways with $v_\parallel/v \lesssim 0.9$.

Runaway driven whistler thresholds have been analyzed [10] for ITER. While the collisionality will become high for the postdisruption phase, such modes can remain unstable if T_e remains above a minimum value. Reference [10] predicts such instabilities are viable for ITER if $T_e >$ 22 eV; this leaves a significant operational range in which runaways can destabilize whistlers.

Nonlinear dynamics.—A typical spectrogram of whistler mode activity is shown in Fig. 7 along with several channels of electron cyclotron emission (ECE) and indicators of low frequency $n = 1$ MHD activity. The signals in Fig. 7(a) show an intermittent behavior, with strong whistler activity over multiple frequency lines, followed by periods with strong suppression. As indicated by the arrows extending from Figs. 7(a) to 7(b), some of the drops in whistler activity are preceded by abrupt increases in the higher frequency ECE amplitudes. Since these ECE channels measure perpendicular energy in moderate energy runaways, the rapid increases are indicative of the nonlinear dynamics of the whistler instability and its feedback on the runaway electron distribution function. It is known from other laboratory and ionospheric measurements that whistlers induce pitch angle scattering of relativistic electrons [8,6].

The remaining drops in whistler amplitude are correlated with $n = 1$ sawtooth activity, as indicated by the gray shaded bars on the lower part of Fig. 7(b). These are associated with opposite variations in the 83.5 and 92.5 GHz channels, implying energy transfers occur from inside to outside of the $q = 1$ surface. The sawtooth correlations imply the runaways are located near $q = 1$ close to the plasma center. Centrally localized runaways were also inferred from bremsstrahlung data.

The question remains as to the role of different regions of the runaway electron phase space in the destabilization and saturation of whistler instabilities. Resonance evaluations (e.g., Fig. 4) show that waves in the measured frequency range of 100 to 200 MHz can be excited either by high energy $v_\parallel/v \sim 1$ runaways through the anomalous Doppler resonance, or by moderate energy low $v_\parallel/v$ runaways through the Cherenkov resonance. The cyclic behavior of Fig. 7 indicates correlations between the perpendicular energy of moderate energy runaways (ECE intensity) and whistler waves. Since the anomalous Doppler resonance couples transit and cyclotron frequencies, it provides a path for conversion from parallel to perpendicular energy. Recent runaway-whistler quasilinear simulations [23] have confirmed that these instabilities can produce nonthermal ECE by anomalous Doppler scattering, although taking into account higher frequency whistlers than those measured here. The extension of these measurements to higher frequencies is a topic for future research.

Conclusions.—Unstable whistler waves driven by runaway electrons have been observed in the DIII-D tokamak in

the 100–200 MHz range. Parametric variations in the wave frequency follow the whistler dispersion relation and instability thresholds are observed that depend on runaway intensity and magnetic field. The wave frequencies are discretized into closely spaced lines related to cavity modes formed by the toroidal periodicity and reflections off the fast wave cutoff regions. Intermittent variations in amplitude can be correlated both with nonlinear scattering of runaways by whistler waves and the effects of sawtooth activity. Relativistic electrons in tokamaks will require improved control methods to avoid damage to plasma-facing components. The whistler wave, runaway interactions studied here have parallels with ionospheric phenomena and are a new mechanism that can influence tokamak runaway generation rates. Also, the potential for scattering runaways by externally launched waves in the observed frequency ranges may lead to new approaches for runaway control.

This work has been supported by the U.S. DOE Frontier Science Program and under the Contracts No. DE-FC02-04ER54698, No. DE-FG02-07ER54917, No. DE-SC0016268, No. DE-AC05-060R23100, No. DE-FG03-94ER54271, No. DE-AC02-09CH11466, and No. DE-AC05-00OR22725. Useful and encouraging discussions with D. C. Pace, N. A. Crocker, Z. Guo, J. H. Harris, and R. J. Buttery have contributed to this effort.

This manuscript has been authored by UT-Battelle, LLC under Contract No. DE-AC05-00OR22725 with the U.S. Department of Energy. The U.S. Government retains and the publisher, by accepting the article for publication, acknowledges that the U.S. Government retains a nonexclusive, paid-up, irrevocable, worldwide license to publish or reproduce the published form of this manuscript, or allow others to do so, for U.S. Government purposes. The Department of Energy will provide public access to these results of federally sponsored research in accordance with the DOE Public Access Plan.

[1] W. H. Preece, Earth currents, Nature (London) **49**, 554 (1894).
[2] R. A. Helliwell, *Whistlers and Related Ionospheric Phenomena* (Dover, New York, 2006).
[3] B. E. Carlson, N. G. Lehtinen, and U. S. Inan, Runaway relativistic electron avalanche seeding in the Earth's atmosphere, J. Geophys. Res. **113**, A10307 (2008).
[4] Y. Y. Shprits, D. A. Subbotin, N. P. Meredith, and S. R. Elkington, Review of modeling of losses and sources of relativistic electrons in the outer radiation belt. Part II. Local acceleration and loss, J. Atmos. Sol. Terr. Phys. **70**, 1694 (2008).
[5] R. B. Horne and R. M. Thorne, Relativistic electron acceleration and precipitation during resonant interactions with whistler-mode chorus, Geophys. Res. Lett. **30**, 1493 (2003).
[6] A. Varotsou, D. Boscher, S. Bourdarie, R. B. Horne, N. P. Meredith, S. A. Glauert, and R. H. Friedel, Three-dimensional test simulations of the outer radiation belt electron dynamics including electron-chorus resonant interactions, J. Geophys. Res. **113**, A12212 (2008).
[7] R. L. Stenzel, J. M. Urrutia, and K. D. Strohmaier, Whistler Instability in an Electron Magnetohydrodynamic Spheromak, Phys. Rev. Lett. **99**, 265005 (2007).
[8] B. Van Compernolle, J. Bortnik, P. Pribyl, W. Gekelman, M. Nakamoto, X. Tao, and R. M. Thorne, Direct Detection of Resonant Electron Pitch Angle Scattering by Whistler Waves in a Laboratory Plasma, Phys. Rev. Lett. **112**, 145006 (2014).
[9] T. Fülöp, G. Pokol, P. Helander, and M. Lisak, Destabilization of magnetosonic-whistler waves by a relativistic runaway beam, Phys. Plasmas **13**, 062506 (2006).
[10] P. Aleynikov and B. Breizman, Stability analysis of runaway-driven waves in a tokamak, Nucl. Fusion **55**, 043014 (2015).
[11] V. S. Vlasenkov, V. M. Leonov, V. G. Merezhkin, and V. S. Mukhovatov, The runaway electron discharge regime in the tokamak-6 device, Nucl. Fusion **13**, 509 (1973).
[12] V. V. Alikaev, K. A. Razumova, and Yu. A. Sokolov, Runaway-electron instability in the TM-3 tokamak, Sov. J. Plasma Phys. **1**, 303 (1975).
[13] H. Drieicer, Electron and Ion Runaway in a Fully Ionized Gas II, Phys. Rev. **117**, 329 (1960).
[14] J. W. Connor and R. J. Hastie, Relativistic limitations on runaway electrons, Nucl. Fusion **15**, 415 (1975).
[15] M. N. Rosenbluth and S. V. Putvinski, Theory for avalanche of runaway electrons in tokamaks, Nucl. Fusion **37**, 1355 (1997).
[16] J. R. Martin-Solis, J. D. Alvarez, R. Sanchez, and B. Esposito, Momentum–space structure of relativistic runaway electrons, Phys. Plasmas **5**, 2370 (1998).
[17] M. Lehnen, K. Aleynikova, P. B. Aleynikov, and D. J. Campbell, Disruptions in ITER and strategies for their control and mitigation, J. Nucl. Mater. **463**, 39 (2015).
[18] R. S. Granetz, B. Esposito, J. H. Kim, R. Koslowski, M. Lehnen, J. R. Martin-Solis, C. Paz-Soldan, T. Rhee, J. C. Wesley, and L. Zeng, An ITPA joint experiment to study runaway electron generation and suppression, Phys. Plasmas **21**, 072506 (2014).
[19] C. Paz-Soldan, C. M. Cooper, P. Aleynikov, D. C. Pace, N. W. Eidietis, D. P. Brennan, and R. S. Granetz, E. M. Hollmann, C. Liu, A. Lvovskiy, and R. A. Moyer, D. Shiraki, Spatiotemporal Evolution of Runaway Electron Momentum Distributions in Tokamaks, Phys. Rev. Lett. **118**, 255002 (2017).
[20] C. Paz-Soldan, N. W. Eidietis, R. S. Granetz, E. M. Hollmann, R. A. Moyer, N. A. Crocker, A. Wingen, and Y. Zhu, Growth and decay of runaway electrons above the critical electric field under quiescent conditions, Phys. Plasmas **21**, 022514 (2014).
[21] C. Paz-Soldan, C. M. Cooper, P. Aleynikov, N. W. Eidietis, A. Lvovskiy, D. C. Pace, D. P. Brennan, E. M. Hollmann, C. Liu, R. A. Moyer, and D. Shiraki, Resolving runaway electron distributions in space, time, and energy, Phys. Plasmas **25**, 056105 (2018).
[22] E. F. Jaeger, L. A. Berry, E. D'Azevedo, D. B. Batchelor, and M. D. Carter, All-orders spectral calculation of radio-frequency heating in two-dimensional toroidal plasmas, Phys. Plasmas **8**, 1573 (2001).
[23] C. Liu, Ph.D. thesis, Princeton University, Princeton, NJ, 2017.